Appl Magn Reson (2011) 40:567–580
DOI 10.1007/s00723-011-0239-z

Applied
Magnetic Resonance

Electron Spin Resonance Study on the Photoinduced Electron Transfer in Chlorophyll a in Reconstituted Lipid Bilayer Vesicles

Chang Woo Kim · Don Keun Lee · Young Soo Kang

Received: 22 November 2010 / Revised: 28 May 2011 / Published online: 28 June 2011

Abstract The photoinduced electron transfer from chlorophyll a through the interface of positively charged dioctadecyltrimethylammonium chloride (DODAC), neutral dipalmitoylphosphatidylcholine (DPPC) and negatively charged dihexadecylphosphate (DHP) headgroup of the lipid bilayers was studied. The photoinduced radicals were identified by electron spin resonance (ESR) and radical yields of chlorophyll a were determined by double integration of the ESR spectra. The formation of vesicles was identified indirectly by measuring change of the λ_{max} value of optical absorption spectrophotometer from diethyl ether solution to vesicle solutions, and observed directly with scanning and transmission electron microscopic images. The interaction distance between chlorophyll a and interface water (D_2O) determined by deuterium modulation depth with electron spin echo modulation (ESEM) showed a decreasing order DODAC > DPPC > DHP. The interface charge of each vesicle was determined with zeta potential measurement. The interface charge of the lipid bilayers affected the radical yields of chlorophyll a more critically than the interaction distance between chlorophyll a and interface water.

1 Introduction

Photosynthesis has long been a subject of extensive studies by research workers in diverse fields of physical and biological sciences [1–4]. Those aspects involved in this process in bioenergetics have been studied with the hope of elucidating, among other things, the mechanism of the primary events of photosynthesis by electron

C. W. Kim · Y. S. Kang (✉)
Department of Chemistry, Sogang University, Shinsu-dong #1,
Mapo-gu, Seoul 121-742, Korea
e-mail: yskang@sogang.ac.kr

D. K. Lee
Department of Chemistry, Pukyong National University,
Daeyeon-3-dong, Nam-gu, Busan 608-737, Korea

transfer process, which is initiated by photoexcitation of chlorophyll a in the photosynthetic reaction center. The ultimate results of light-induced electron transfer process in green plants are the oxidation of water and the fixation of CO_2 into carbohydrate, thereby storing a significant fraction of the absorbed electromagnetic energy in the form of chemical bond energy.

An understanding of the details of photoinduced electron transfer across lipid bilayer membranes of plants is crucial to the rational design of artificial photosynthetic devices that relay on bilayer membranes to mediate charge separation. This is a model system of the natural photosynthesis occurring in leaves of plants and involves the light energy conversion into chemical energy by suppressing back electron transfer reaction between an electron donor and an electron acceptor. Previous studies already reported on the photoinduced electron transfer from several kinds of organic electron donors to their corresponding electron acceptors across the interface of the vesicles or micelles [5–15]. One approach to light energy conversion into chemical and electrical energy involves photoionization of photosensitive organic molecules in organic molecular assemblies. Such a process results in a charge-separated state containing potential energy converted from light energy. Optimization of photoinduced charge separation has been achieved by control of the photosensitive chromophore location and the interface charge of the molecular assemblies [8, 9]. The control of interface charge of the molecular assemblies has been accomplished by variation of the surfactant molecules with differently charged headgroups [10, 16–20]. The control of distance between the electron donor and acceptor has been achieved by changing the alkyl chain length of the photosensitive molecules and by adding cosurfactants such as cholesterol, ureas and alcohols [21–24]. The net photoionization efficiency is enhanced over homogeneous solutions by the localization of the photosensitive molecules within surfactant assemblies.

The net photoionization efficiency can be determined by the yield of the cation radical of molecules or their converted products. In frozen systems, this can be measured by electron spin resonance (ESR). The location of the photosensitive moiety relative to a surfactant assembly interface can be determined by the deuterium modulation depth of electron spin echo modulation (ESEM) of the photoinduced cation in surfactant assemblies prepared in deuterated water [16, 25].

Such electron magnetic resonance studies have been carried out in frozen state because the lifetimes of photoinduced radical cations are short at room temperature and the exploitation of ESEM to measure weak dipolar interactions requires solid-state systems [8, 26, 27]. Hence, the molecular assemblies are frozen rapidly to make such an analysis possible. Numerous studies have demonstrated that the micellar and vesicular structure is retained in rapidly frozen aqueous solutions [25, 28–31].

In previous studies with photosensitive porphyrin derivatives, the localization and photoionization of a series of (alkylpyridyl)triphenylporphyrin derivatives were investigated in vesicular and reverse micellar systems in the frozen system at 77 K [11, 32]. The relative location of the photosensitive moiety of an electron donor such as porphyrins was controlled relative to the assembly interface by changing pendant alkyl chain lengths and by perturbing the interface structure of the molecular assemblies. Also, the energy barrier for the electron transfer through the

interface was modified by perturbing the interface structure and by changing the interface charge. This was carried out by adding surface-active molecules into the molecular assemblies and changing kinds of molecular assemblies, which have intrinsic interface charge such as positive, neutral and negative.

In the present study, chlorophyll a was solubilized into anionic dihexadecylphosphate (DHP), neutral dipalmitoylphosphatidylcholine (DPPC) and cationic dioctadecyldimethylammonium chloride (DODAC) vesicular solution and photoionized by light irradiation. The solubilization of chlorophyll a into the vesicular solution was identified on an ultraviolet–visible (UV–Vis) spectrophotometer. The photoinduced cation radicals of chlorophyll a and other radicals induced by radical conversion were identified by ESR and the electron transfer efficiency can be monitored by double integration of the ESR spectra of the photoinduced cation radicals and their reaction product radicals if any. Such a work was carried out in the frozen state at 77 K to preserve the photoinduced radical cations because of its short lifetime at room temperature. There is still a lot of controversy on the structure retaining several kinds of molecular assemblies such as micelles and vesicles. To demonstrate whether the vesicular structure is retained in rapidly frozen aqueous solutions, their images were checked with cryo-transmission electron microscopy (TEM) and scanning electron microscopy (SEM). The interaction distance between chlorophyll a and interface water (D_2O) was determined by deuterium modulation depth with ESEM. The photoinduced cation radical yields of chlorophyll a in the various interface charge vesicles were studied by determining the amount of radical yields on the basis of the interface charge of vesicles. In the present study, we first determined the interface charge of the vesicles by determining zeta potentials of vesicles. This gives the direct evidence of the relation between the amounts of the cation radical of chlorophyll a induced by electron transfer through the interface of vesicles.

2 Experimental

2.1 Materials

Chlorophyll a and b were extracted from fresh spinach leaves by the conventional method. Their structure was identified on Fourier-transform nuclear magnetic resonance (FT-NMR, JEOL, JNM-ECP 400), Fourier-transform infrared (FT-IR, Bruker, IFS-88) and chemical luminescence specrophotometer (Perkin-Elmer, HTS 7000 Plus). Its purity was determined to be 99% from its extinction coefficient in diethyl ether at 660 nm versus the literature value of 8.6×10^{-4} M^{-1} cm^{-1} [33]. DHP and DPPC were obtained from Sigma Chemical Co. and used without further purification. Dioctadecyldimethylammonium bromide (DODAB) was purified from Eastman Kodak and purified by recrystallization from acetone. A methanol–chloroform (70:30, v/v) solution of DODAB was passed through a dilute ion exchange resin, type AG 2×8, 20–50 mesh Biorad Laboratories, to form dioctadecyldimethylammonium chloride (DODAC). The eluent containing DODAC was evaporated, and the solid residue was recrystallized two times from acetone–water (95:5, v/v). Tri(hydoxymethyl)aminomethane (Tris, Gold Label, 99.9+%)

and 2 M hydrochloric acid were purchased from Aldrich and Sigma Chemical Co., respectively. Distilled water was passed through a six-cartridge Barnstead Nanopure II purification train with a Macropure pretreatment. Organic solvents, such as chloroform and methanol, were either spectroanalyzed or of high performance liquid chromatography (HPLC) grade. Buffer solutions were prepared with sodium phosphate, sodium pyrophosphate and sodium ethylene diaminetetraacetate (EDTA) from Aldrich Chemicals. The molecular structures of chlorophyll a and b, and lipids of DHP, DODAC and DPPC are shown in Fig. 1.

2.2 Sample Preparations

Stock 30 mM solutions of vesicle surfactants (DPPC, DHP and DODAC) were prepared in chloroform. The stock solution of chlorophyll a was also prepared in chloroform. The exact concentration was measured with optical absorption spectroscopy on a Varian CARY 1C UV–Vis spectrophotometer ($\lambda_{max} = 423$ nm in chloroform, $\log\varepsilon = 3.71$ M^{-1} cm^{-1}) [33]. For the preparation of DODAC or DPPC vesicle solutions, 0.6 ml of a 0.1 M vesicle stock solution and 70 μl portions of 10 mM chlorophyll a stock solution in chloroform were transferred into a test tube. Chloroform was evaporated under a stream of nitrogen gas. Then, 1 mL of distilled water was added to the DODAC and DPPC thin films. The resulting solutions were sonicated for 20 min at 53 ± 2°C under nitrogen gas using Fisher 300 sonic dismembrator operated at 35% relative output through a tungsten microtip with an outer diameter of 4 mm to form completely solubilized clear solutions. The formation of vesicles containing chlorophyll a was identified indirectly by measuring λ_{max} value change from diethyl ether solution to vesicle solutions. Optical absorption spectra were measured in 1 cm path length quartz cell at room temperature. Then, 100 μl of each sample solution was placed into a Suprasil quartz tube with an inner diameter of 2 mm and outer diameter of 3 mm, which was flame sealed at one end. The tubes were shaken to equilibrate the solution and then the samples were sealed to prevent evaporation loss and to minimize contact with oxygen. The samples were rapidly frozen by plunging into liquid nitrogen. The morphologic analysis of the frozen vesicles was carried out by SEM (Hitachi

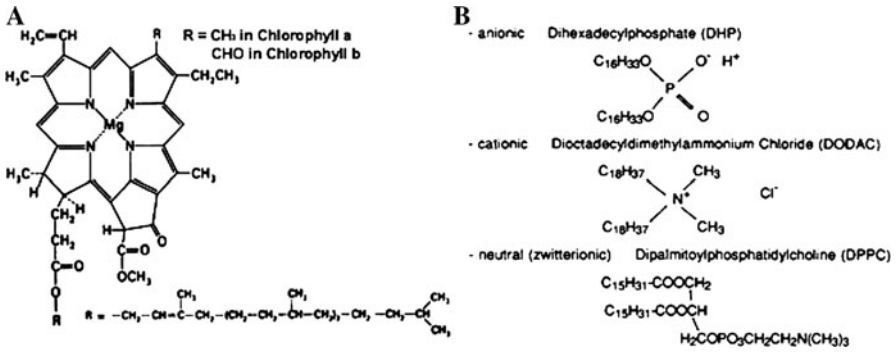

Fig. 1 Molecular structures of chlorophylls (a and b) and lipids (DHP, DODAC and DPPC)

S-4200 FE-SEM) after coating the sample with Pt, and by TEM (JEOL TEM-2010) after staining the sample with uranyl acetate (2%), respectively.

2.3 Photoirradiation

Photoirradiation of the frozen samples of chlorophyll a in vesicles was carried out at 77 K with a 300-W xenon lamp (ILC-LX 300 UV). A 10 cm water filter and a Corning No. 5030 band pass filter for blue-light irradiation (300 nm, $\lambda_{irr} < 558$ nm) were placed in the light path to give 80% transmittance at 423 nm. The photoyield of the chlorophyll a cation radical was measured by the irradiation time of photolysis. The light intensity at the sample position was measured with a YSI-Kettering model 65 radiometer and was 0.882×10^3 W m^{-2}. The Dewar holding the sample tube was rotated at 4 rpm during photolysis to ensure even irradiation of the sample.

2.4 Magnetic Resonance Experiments

ESR spectra were recorded at X-band on a JEOL JEX-FX 200-300 spectrometer. The irradiated sample cell was placed in a quartz ESR Dewar (Wilmad Glass Co.), which was filled with liquid nitrogen and secured in a TE_{104} cavity. The loaded Q factor of this cavity was measured at about 1800. The finger of the Dewar was placed at the microwave magnetic field maximum. The microwave power was maintained at 1.97 mM, which was well below the saturation level of the irradiated chlorophyll a sample solution. The standard spectrometer settings used in ESR experiments were as follows: modulation field amplitude, 0.281 mT; sweep width, 20 mT; number of accumulations, 7 scans; scan time constant, 56 s; microwave frequency, 9.503 GHz; and receiver gain, 1.23×10^5. The photoinduced cation radical yield of chlorophyll a was determined in triplicate for each system by double integration of the ESR spectra using the JEOL JES-EM software. The normalized photoyield values were obtained by dividing the photoyield of the chlorophyll a/DODAC/H_2O system. Mn^{+2} in MgO was used as a magnetic field marker.

Two-pulse ESE signals were recorded at 4.2 K on a Bruker ESP380 X-band ESR spectrometer [26, 27]. The microwave pulse widths used were 40 and 80 ns. Each signal was scanned ten times. The deuterium modulation was characterized by a 0.5 ms periodicity. Once obtained, the ESE data were transferred to an IBM-compatible 586 based microcomputer for later, off-line analysis. The deuterium modulation depths were normalized by dividing the depth at the first modulation minimum by the depth to the base line at the same interpulse time [26, 27]. The simulation of the ESE signal was carried out with ESFT software by fitting the isotropic coupling constant ($A_{iso} = 0.1$ MHz), the dipolar interaction distance (R) and the number of nuclei interacting with the unpaired electron (N).

3 Results and Discussion

The structure of the isolated chlorophyll a and b were identified with fluorescence and UV–Vis spectroscopies. The optical absorption and fluorescence emission

bands are consistent with the previous reports [33, 34]. The structure of chlorophyll a and b are also identified with FT-NMR and FT-IR and the results are consistent with previous reports [35]. To identify the incorporation of chlorophyll a into the interface of the vesicles, the optical absorption of chlorophyll a was in the diethylether, and DHP, DPPC and DODAC vesicles were measured and the results are shown in Fig. 2. There is no optical absorption band in vesicle solution only. A red shift of 11 nm of the absorption bands of chlorophyll a at $\lambda_{max} = 671$ in the vesicle solution from the band at $\lambda_{max} = 660$ in diethylether solution might be caused by different environmental interactions of chlorophyll a [36]. In the vesicle solutions of chlorophyll a, an absorption band at around 685 nm was assigned to aggregated chlorophyll a into the vesicle interface [37]. The formation of hydrated chlorophyll a polymer has been reported to give an absorption band at 740 nm [38]. Since there are no absorption bands at 740 or 685 nm in our prepared samples, we conclude that chlorophyll a is solubilized in its monomeric form in our samples. The red shift of 10 nm indicates that the chlorine ring is located in a polar environment near the surfactant headgroup region and possibly exposed to the aqueous environment.

Figure 3 shows the SEM images of DODAC vesicle and DODAC vesicle containing chlorophyll a at 77 K. The shape and structure of DODAC were well preserved even in the frozen state at 77 K. Even after chlorophyll a was solubilized into the DODAC vesicle, the shape and structure were well preserved and not affected by the chlorophyll a addition. There is yet much controversy on retaining the vesicle or micelle structure by the change of temperature to the frozen state at 77 K and the addition of surface-active agents into the vesicle solutions [5–8, 21–25]. The same trend was found in the samples with DHP vesicle with SEM image measurement and with DPPC vesicle with TEM image measurement as shown in Figs. 4 and 5, respectively.

On the basis of retaining the vesicle structure in the frozen state of the sample at 77 K, the photoinduced cation radical of chlorophyll a was determined by the

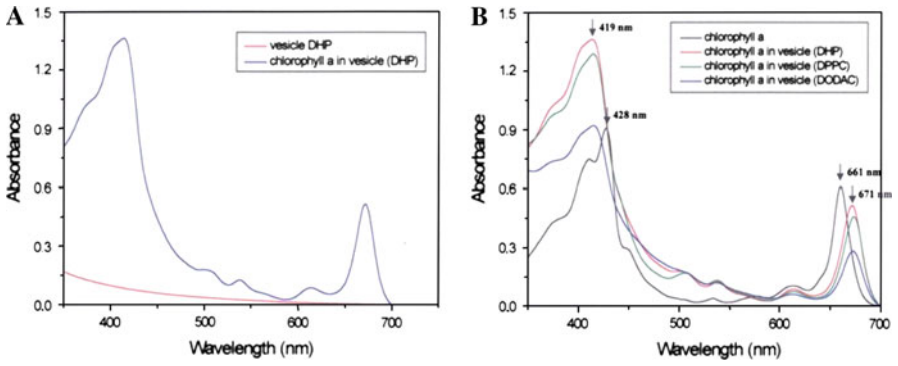

Fig. 2 Optical absorption spectra of 1×10^{-3} M DHP vesicles and 3×10^{-5} M chlorophyll a in DHP vesicles (**a**) and 3×10^{-5} M chlorophyll a in diethyl ether, DHP vesicles, DPPC vesicles and DODAC vesicles (**b**)

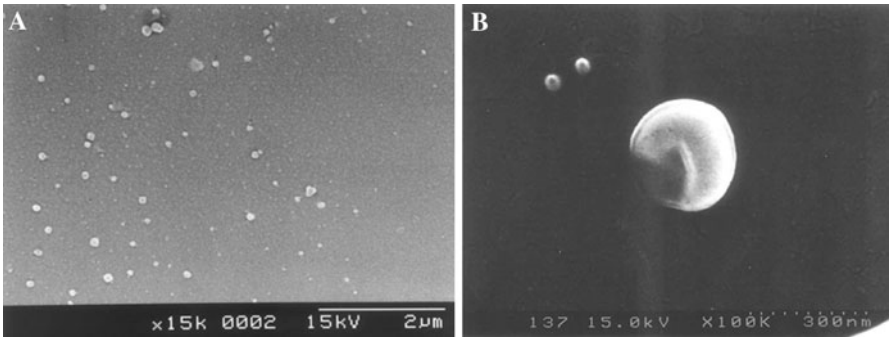

Fig. 3 SEM images of 1×10^{-3} M DODAC vesicles (**a**, ×10,000) and 1×10^{-3} M DODAC vesicles containing 3×10^{-5} M chlorophyll a (**b**, ×100,000) at 77 K. The size of vesicles was 80–180 nm

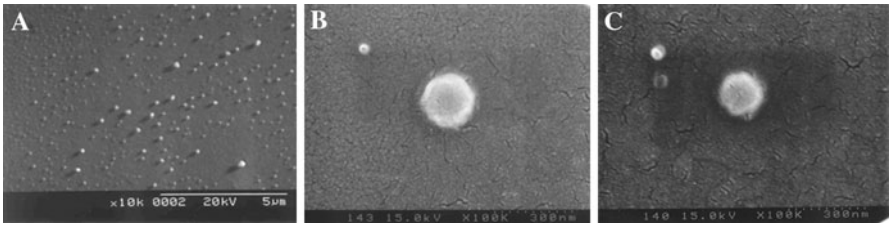

Fig. 4 SEM images of 1×10^{-3} M DHP vesicles (**a**, ×10,000 and **b**, ×100,000), 1×10^{-3} M DHP vesicles containing 3×10^{-5} M chlorophyll a (**c**, ×100,000) at 77 K. The size of vesicles is 80–180 nm

double integration of the ESR spectra. Photoirradiated samples without chlorophyll a showed no ESR signals. This indicates that chlorophyll a is the only photosensitive material in these systems. For the photoinduced charge separation of chlorophyll a solubilized into the vesicle solutions, photoinduced electron transfer occurs from chlorophyll a to the interface water through the vesicle interface. This is schematically shown in Fig. 6. To obtain the maximum yields of photoinduced cation radical of chlorophyll a, the interface structure and interface charge were modified by changing kinds of vesicles and adding surface-active agents such as chlolesterol, urea, etc., in the previous reports [20–22].

The functions of the vesicle interface are to keep the optimum electron transfer distance between the electron donor and acceptor and to control the optimum energy barrier of electron transfer through the interface. Figure 7 shows the first-derivative X-band ESR spectra of chlorophyll a in DHP, DODAC and DPPC vesicles. The photoinduced cation radical of chlorophyll a was identified with a *g*-factor of 2.0026 [18, 19].

Figure 8 shows the data on the normalized photoyields of cation radical of chlorophyll a on the molar ratio of chlorophyll a to DPPC in frozen vesicles. The photoyield of chlorophyll a versus the molar ratio of chlorophyll a to DPPC surfactant molecule reached a plateau on the molar ratio of 0.03. This indicates that

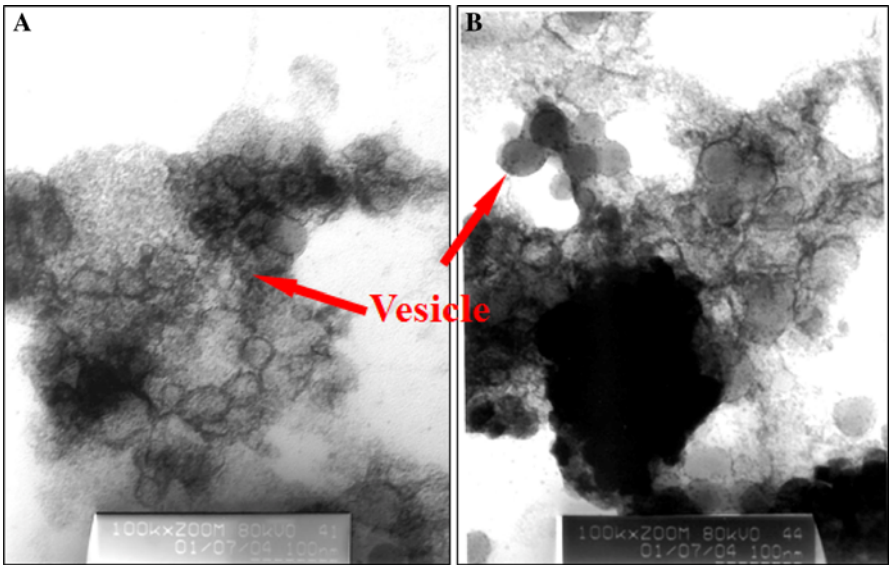

Fig. 5 TEM images of 1×10^{-3} M DPPC vesicles (**a**, ×100,000) and 1×10^{-3} M DPPC vesicle containing 3×10^{-5} M chlorophyll a (**b**, ×100,000) at 77 K after staining with uranyl acetate

the molar ratio of chlorophyll a to DPPC allows the monomeric form of chlorophyll a to be determined as around 0.03 and this resulted in the most efficient photoinduced electron transfer through the interface, not affected by the excess amount of chlorophyll a in the same vesicle. Similar results were obtained with DHP and DODAC vesicles. On the same molar ratio of chlorophyll a to DHP, the normalized photoyield of chlorophyll a versus the photoirradiation time is shown in Fig. 9. The normalized photoyield of chlorophyll a in DHP vesicle determined by the double integration of the first-derivative ESR spectra reached a plateau after 90 min of photoirradiation. This indicates that the intensity of ESR spectra of chlorophyll a/vesicle/H_2O samples after 90 min of photoirradiation can be relatively compared on the effect by the various kinds of vesicles.

Figure 10a shows the normalized photoyields of chlorophyll a/vesicle/H_2O samples after 90 min of photoirradiation. Figure 12 shows the ESEM signals of chlorophyll a cation radical in DHP, DPPC and DODAC vesicles. The frequency of this modulation is characteristic of an interaction of an unpaired electron with a deuterium nucleus. ESEM shows the degree of interaction between the unpaired electron on the aromatic rings of the chlorophyll a cation and the surrounding deuterium nuclei located within a distance of around 0.6 nm [8, 26]. This modulation arises as a result of dipole–dipole interactions, which are averaged out in the solid samples.

The period of the modulation on the ESE decay envelope is proportional to the reciprocal of the magnetogyric ratio and is characteristic of the type of nuclei present in the microenvironment of the radical within 0.6 nm. The modulation depth

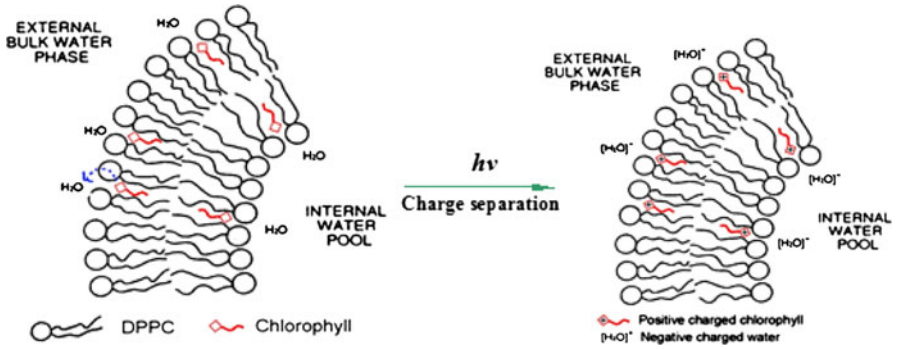

Fig. 6 Schematic representation of the charge separation of chlorophyll a in DPPC vesicles by photoirradiation

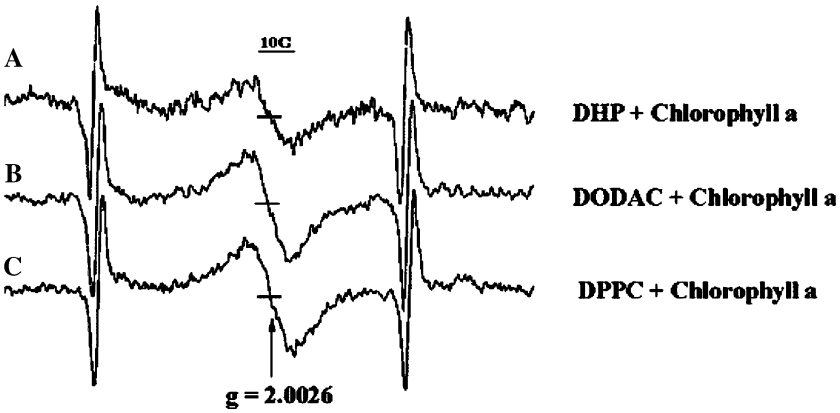

Fig. 7 First-derivative X-band ESR spectra of chlorophyll a in DHP vesicles (**a**), DODAC vesicles (**b**) and DPPC vesicles (**c**). The spectra were recorded at 77 K after 90 min blue-light irradiation (300 nm $< \lambda_{irr} <$ 558 nm). The *sharp lines* on both sides of the spectra are from Mn^{2+} in MgO used as a magnetic field marker

depends on both the number of and mean distance to these nuclei. Therefore, a change in modulation depth can result from either a change in the average distance or the number of nuclei, or both. Deuterium modulation depths of samples show the decreasing order DHP > DPPC > DODAC. The more correct data on the interaction distance were obtained with the simulated curves on the assumption that the number of interacting deuterium nuclei of interface water (D_2O) and isotropic coupling constant were fixed at the same values as $N = 4$ and $A_{iso} = 0.1$ MHz, respectively.

The results show the interaction distance between the cation radical of chlorophyll a and interface water (D_2O) as 0.412 nm in DPDAC, 0.393 nm in DPPC and 0.375 nm in DHP. This indicates that the interaction distance between photoinduced cation radical and deuterium nuclei in the interface water (D_2O) was the longest in DODAC, then decreased at DPPC and finally was the shortest at DHP.

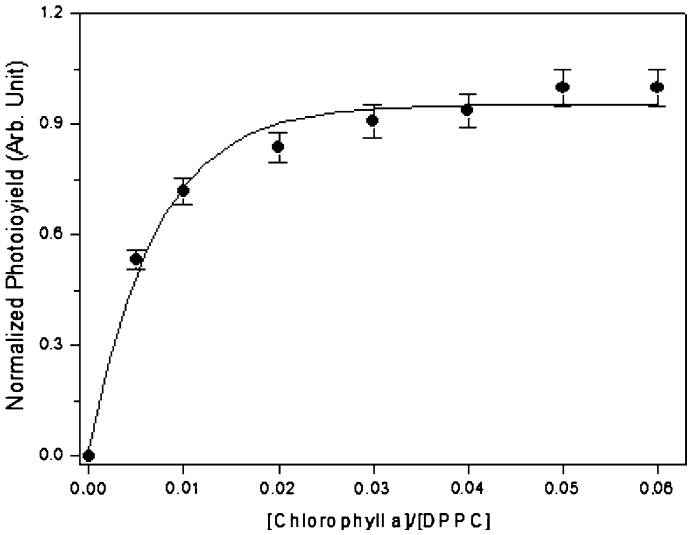

Fig. 8 Dependence of the normalized photoyield of chlorophyll a upon the molar ratio of chlorophyll a to DPPC in DPPC frozen vesicles. Photoirradiation was carried out with blue light (300 nm $< \lambda_{irr} <$ 558 nm) for 10 min at 77 K

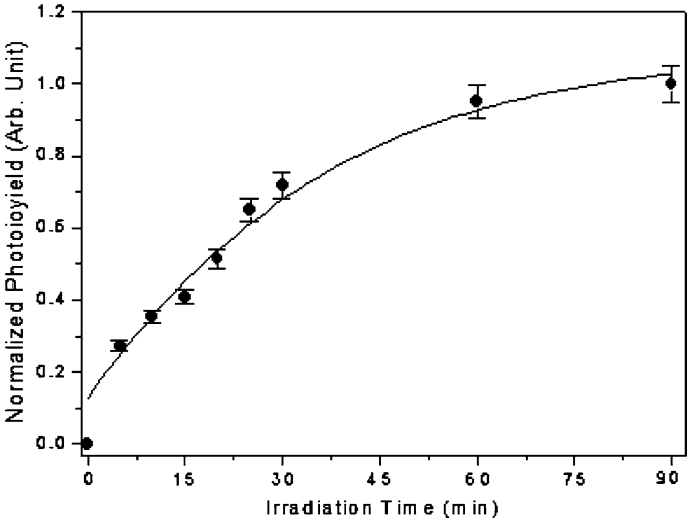

Fig. 9 Dependence of the normalized photoyield of chlorophyll a/DHP vesicle samples versus the irradiation time of the blue-light irradiation (300 nm $< \lambda_{irr} <$ 558 nm) in the frozen state at 77 K. [Chlorophyll a]/[DHP] molar ratio is 0.03

This is interpreted as: chlorophyll a cannot penetrate into the headgroup region of DHP vesicle because of compact headgroup structure and thus results in the short interaction distance between chlorophyll a cation and interface water (D_2O) of the DHP vesicle. Their interaction distance slightly increases in DPPC vesicle and is the

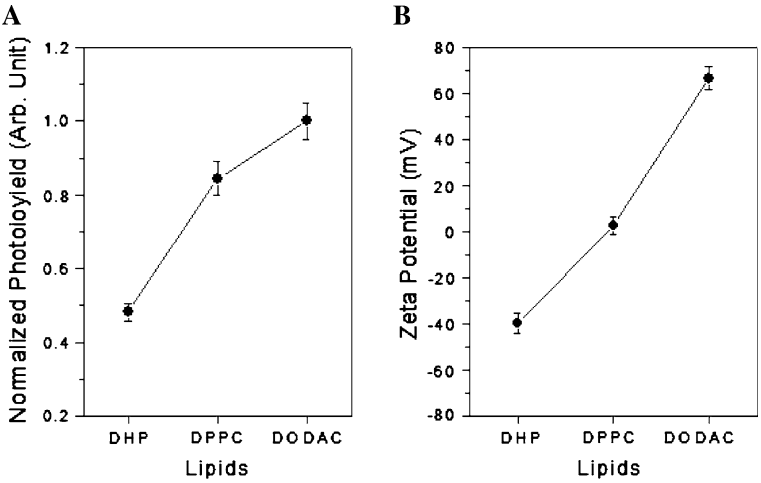

Fig. 10 Dependence of the normalized photoyield of chlorophyll a upon the kind of lipids (**a**) and zeta potential of vesicles containing chlorophyll a (**b**) at 77 K. [Chlorophyll a]/[lipid] molar ratio is 0.03

longest in the DODAC vesicle because a bulky headgroup of DODAC monomer allows chlorophyll a to be buried deeper in the DODAC vesicle. Even with shorter interaction distance between chlorophyll a and interface water (D_2O), the photoyields of chlorophyll a in vesicles are in the order DODAC > DPPC > DHP as shown in Fig. 10a. The interfacial potential determined as interface charge of the vesicles, as shown in Fig. 11, plays an important role in determining the net charge separation. The photoyield was higher in cationic versus anionic vesicles. This can be interpreted by a deceasing energy barrier for the electron transfer through the vesicular interface in the order DHP > DPPC > DODAC. The cationic interface charge of vesicles gives higher photoyields even with a greater interaction distance between chlorophyll a and interface water (D_2O). The interface charges of vesicles are determined with zeta potential measurement and are shown in Fig. 10b. The measured zeta potential of vesicle interfaces shows a positively charged interface of DODAC as 63 mV, neutral interface charge of DPPC and negatively charged interface charge of DHP as −40.2 mV. This allows the consistent energy barrier for the electron transfer through the interface of vesicles and results in the order of photoyield as DODAC > DPPC and DHP as shown in Fig. 10a. Schematic representation of negatively charged DHP vesicles, neutral DPPC vesicles and positively charged DODAC vesicles is demonstrated in Fig. 11. In the previous report [39], even with the shorter electron transfer distance between phenothiazine solubilized in the DHP, DPPC and DODAC vesicles and interface water of vesicles, the interface charge of vesicles critically controlled the photoyields of phenothiazine by the different interface charge of vesicles in decreasing order DODAC > DPPC > DHP, as shown in Fig. 12. The consistent result in the present study indicates that the most important parameter for the photoinduced charge separation of chlorophyll a in vesicles is the interface charge of vesicles.

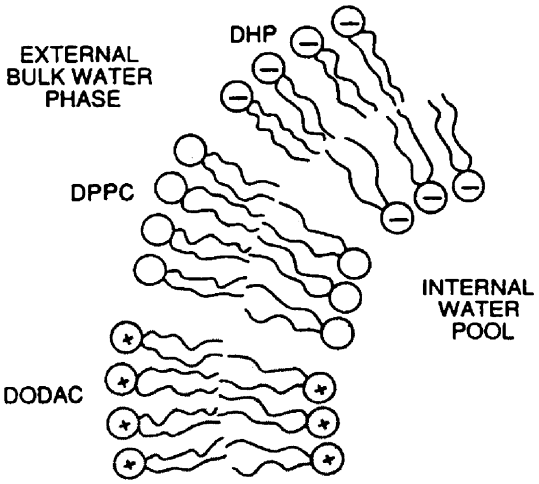

Fig. 11 Schematic representation of negatively charged DHP vesicles, neutral DPPC vesicles and positively charged DODAC vesicles

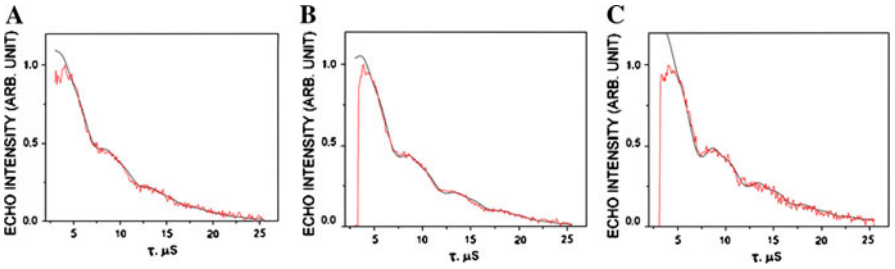

Fig. 12 Two-pulse X-band ESE signals of chlorophyll a in **a** DODAC/D_2O vesicles, **b** DPPC/D_2O vesicles and DHP/D_2O vesicles at 4 K. Experimental (*continuous line*) and computer-simulated (*dotted line*) signals are shown with fitting parameters of **a** $N = 4$, $R = 0.412$ nm and $A_{iso} = 0.1$ MHz, **b** $N = 4$, $R = 0.393$ nm and $A_{iso} = 0.1$ MHz, and **c** $N = 4$, $R = 0.375$ nm and $A_{iso} = 0.1$ MHz

The study on the photoyield measurement of chlorophyll a in frozen vesicles is possible by identifying the retained structure of vesicles at 77 K and even after incorporation of chlorophyll a into the vesicle solutions. The photoyield depends on the vesicle interface charge and decreases in the order DODAC > DPPC > DHP. This can be interpreted by a deceasing energy barrier for the electron transfer through the vesicular interface in the order DHP > DPPC > DODAC. The interface charge of vesicles was determined with zeta potential measurement and is shown in Fig. 10b. The measured zeta potential of vesicle interfaces shows a positively charged interface of DODAC as 63 mV, neutral interface charge of DPPC and negatively charged interface charge of DHP as −40.2 mV. This allows the consistent energy barrier for the electron transfer through the interface of vesicles and results in the order of photoyield as DODAC > DPPC and DHP. In the previous report [39], even with the shorter electron transfer distance between phenothiazine solubilized in the DHP, DPPC and DODAC vesicles and interface water of vesicles, the interface charge of vesicles critically controlled the photoyields of

phenothiazine by the different interface charges of vesicles in decreasing order as DODAC > DPPC > DHP. The consistent result in the present study indicates that the most important parameter for the photoinduced charge separation of chlorophyll a in vesicles is the interface charge of vesicles. The first measurements of the interface charge of the vesicles were carried out with zeta potential measurement in the present study. The study on the photoyield measurement of chlorophyll a in frozen vesicles is possible by identifying the retained structure of vesicles at 77 K and even after incorporation of chlorophyll a into the vesicle solutions.

4 Conclusions

The efficiency of photoinduced electron transfer of chlorophyll a solubilized into the positively charged DODAC, neutral DPPC and negatively charged DHP vesicles was studied by ESR by integration of the first-derivative ESR spectra. This was carried out on the basis of the identification of chlorophyll a incorporated into the vesicles and the structure retaining of vesicle itself and even after incorporation of chlorophyll a into the vesicles at 77 K. Those identifications were done by the red shift of 11 nm of chlorophyll a from diethylether to aqueous vesicle solutions with UV–Vis spectra and SEM and TEM images at 77 K. The relative photoyields of cationic radical of chlorophyll a in vesicles were obtained in the order DODAC > DPPC > DHP. This is interpreted as: the photoyield is critically affected by the interface charge of vesicles even with longer interaction distance between chlorophyll a and interface water (D_2O). Their interaction distances were determined by deuterium modulation depth measurement. The interface charge provides the energy barrier for the electron transfer through the interface of vesicles. The interface charge of vesicles was determined with zeta potential measurement and was 63 mV of DODAC, neutral of DPPC and −40.2 mV of DHP.

Acknowledgments This work was supported by the Korea Center for Artificial Photosynthesis (KCAP) located in Sogang University and funded by the Ministry of Education, Science and Technology (MEST) through the National Research Foundation of Korea (NRF-2009-C1AAA001-2009-0093879).

References

1. C.A. Wright, R.K. Clayton, Biochim. Biophys. Acta **333**, 246 (1973)
2. A.Y. Borisov, M.D. Illina, Biochim. Biophys. Acta **325**, 240 (1973)
3. L.N.M. Duysens, Brookhaven. Symp. Biol. **11**, 10 (1958)
4. R.T. Ross, M. Calvin, Biophys. J. **7**, 595 (1967)
5. K. Kalyanasundaram, *Photochemistry in Microheterogeneous Systems* (Academic Press, New York, 1987)
6. J.H. Fendler, Acc. Chem. Res. **13**, 7 (1980)
7. J.K. Hurley, G. Tollin, Sol. Energy **28**, 187 (1982)
8. L. Kevan, in *Photoinduced Electron Transfer*, *Part B*, ed. by M.A. Fox (Elsevier, Amsterdam, 1988), pp. 329–384
9. M. Gratzel, *Heterogeneous Photochemical Electron Transfer*, chapt. 1 (CRC, Boca Raton, FL, 1987)
10. M.P. Lanot, L. Kevan, J. Phys. Chem. **93**, 998 (1989)
11. E. de Chastenet Casting, L. Kevan, J. Phys. Chem. **95**, 10178 (1991)

12. Y.S. Kang, P. Baglioni, H.J.D. McManus, L. Kevan, J. Phys. Chem. **95**, 7944 (1991)
13. Y.S. Kang, P. Baglioni, H.J.D. McManus, L. Kevan, J. Phys. Chem. **95**, 7473 (1991)
14. C. Stenland, L. Kevan, J. Phys. Chem. **97**, 5177 (1993)
15. C. Stenland, L. Kevan, J. Phys. Chem. **97**, 10498 (1993)
16. P.A. Narayana, A.S.W. Li, L. Kevan, J. Am. Chem. Soc. **104**, 6502 (1982)
17. E. Rivera-Minten, P. Baglioni, L. Kevan, J. Phys. Chem. **92**, 2613 (1988)
18. T. Hiff, L. Kevan, J. Phys. Chem. **92**, 3982 (1988)
19. D.K. Lee, K.W. Seo, Y.S. Kang, Proc. Indian Acad. Sci. (Chem. Sci.) **114**(6), 533 (2002)
20. P. Bratt, Y.S. Kang, L. Kevan, H. Nakamura, T. Matsuo, J. Phys. Chem. **95**, 6399 (1991)
21. Y.S. Kang, H.J.D. McManus, L. Kevan, J. Phys. Chem. **96**, 10049 (1992)
22. Y.S. Kang, H.J.D. McManus, L. Kevan, J. Phys. Chem. **96**, 10055 (1992)
23. P. Baglioni, L. Kevan, J. Phys. Chem. **91**, 2106 (1987)
24. M.P. Lanot, L. Kevan, J. Phys. Chem. **93**, 5280 (1989)
25. L. Kevan, Int. Rev. Phys. Chem. **9**, 307 (1990)
26. L. Kevan, in *Time Domain Electron Spin Resonance*, ed. by L. Kevan, R.N. Schwartz, chapt. 5 (Wiley, New York, 1990)
27. L. Kevan, in *Modern Pulsed and Continuous Wave Electron Spin Resonance*, ed. by L. Kevan, M.K. Bowman, chapt. 5 (Wiley, New York, 1990)
28. E. Raspaud, B. Pitard, D. Durand, O. Aguerre-Chariol, J. Pelta, G. Byk, D. Scherman, F. Livolant, J. Phys. Chem. B **105**, 52916 (2001)
29. E.T. Kisak, M.T. Kennedy, D. Trommeshauser, J.A. Zasadzinski, Langmuir **16**, 2825 (2000)
30. C.H. Huang, Biochemistry **8**, 344 (1969)
31. F. Bonosi, G. Gabrielli, E. Margheri, G. Martini, Langmuir **6**, 1769 (1990)
32. Y.S. Kang, H.J.D. McManus, K. Liang, L. Kevan, J. Phys. Chem. **98**, 1044 (1994)
33. S. Rong, G. Tollin, Photochem. Photobiol. **47**, 277 (1988)
34. W. Ford, G. Tollin, Photochem. Photobiol. **38**, 441 (1983)
35. W. Stillwell, H.T. Tien, Biochem. Biophys. Res. Comm. **76**, 232 (1977)
36. G.R. Seely, R.G. Jensen, Spectrochim. Acta **21**, 1835 (1965)
37. A.G. Lee, Biochemistry **14**, 4397 (1975)
38. R.G. Brown, E.H. Evans, Photochem. Photobiol. **32**, 103 (1980)
39. Y.S. Kang, H.J.D. McManus, L. Kevan, J. Phys. Chem. **97**, 2027 (1993)